Decay Level Classification of Wooden Components in Tingbao Yang's Former Residence Utilizing Polarization and Fluorescence Effects

Haidi Ji,[#] Yan Yang,[#,*] Hui Zhang, Bin Li, and Lianlong Cheng

Decay levels of wooden components in the Yang former residence were classified using polarized light and fluorescence methods. Analysis of the decay cause was conducted based on external conditions and wood species characteristics. The polarization and fluorescence effects revealed that there were varying degrees of decay in larch (*Larix potaninii* var. *australis*), spruce (*Picea brachytyla*), lace-bark pine (*Pinus bungeana*), Masson pine (*Pinus massoniana*), Chinese Douglas fir (*Pseudotsuga sinensis*), Chinese fir (*Cunninghamia lanceolata*), poplar (*Populus tomentosa*), and elm (*Ulmus pumila*). The primary factors contributing to decay included the inherent low natural durability of the wood species and adverse external conditions, such as damaged roofs, missing dripping water and tiles causing water leakage, uneven indoor and outdoor ground levels, contemporary tile paving indoors, and inadequate ventilation. This study aims to establish a scientific basis for subsequent conservation strategies.

DOI: 10.15376/biores.19.3.4087-4103

Keywords: Ancestral wooden homes; Wood rot; Wooden components; Polarization; Fluorescence effects; Decay cause

*Contact information: School of Architecture, Nanyang Institute of Technology, Nanyang City, Henan Province, 473000, P.R. China; * Corresponding author: yangyanrainy@163.com*

INTRODUCTION

The focus of this study, located in the western section of Jiefang Road, Wancheng District, Nanyang City, Henan Province, was the ancestral home of Mr. Tingbao Yang, a distinguished contemporary Chinese architect. The buildings were constructed during the late Qing Dynasty, and include the Yang family courtyard, Xu family courtyard, Taigu Sugar Company, and the Yang family back pit.

The residence is considered one of the most well-preserved residential buildings in Nanyang City, bearing witness to the struggles of modern revolutionaries from the Xinhai Revolution to the New Democracy Revolution, and showcasing a wealth of folk cultural connotations and exemplifying the urban living style prevalent in southwestern Henan Province during the late Qing Dynasty. It provides valuable insights into life conditions, folk customs, and manners of local people during the late Qing Dynasty Republic era. The well-preserved courtyards exhibit a complete architectural style and hold high conservation value.

Although preservation efforts have been ongoing for Tingbao Yang's former residence, the key load-bearing wooden components, such as columns, beams, lintels, purlins, and rafters, have suffered extensive deterioration, worm damage, and cracks. The degradation of wood inevitably leads to alterations in the anatomical structure of wood cell

walls and degradation of chemical components (Cavallaro *et al.* 2017; Tamburini *et al.* 2017; Bari *et al.* 2019, 2020; Dong *et al.* 2020; Yang *et al.* 2020, 2021a,b, 2022a,b,c; Broda *et al.* 2022). As the degree of deterioration increases, there is a noticeable attenuation in the physical and mechanical properties (Brischke *et al.* 2019; Ueda *et al.* 2020). It is widely acknowledged that the health condition of load-bearing wooden components directly impacts the safety of a wooden frame. Any issues with the wood frame pose a significant threat to the overall stability of the building structure.

As a result, the accurate and scientific detection and diagnosis of wooden components have become a top priority in assessing ancient wooden buildings. Non-destructive testing methods (Chang *et al.* 2016; Dai *et al.* 2017; Zhang *et al.* 2021), such as stress wave detection, resistance meter detection, and ultrasonic detection, can be utilized to evaluate the internal health condition or material performance without destroying the original shape and structure of wooden components. However, this method still remains a macro-scale detection technique that can only offer a more comprehensive qualitative or quantitative assessment of deteriorated phenomena in severely damaged areas. It presents challenges in scientifically identifying the initiation of cell wall microstructure degradation within regions diagnosed as "healthy" at the macro level.

Polarized microscopy can be utilized to assess the distribution and composition of cellulose crystal zones within wood cell walls. The birefringence brightness of crystalline cellulose (BBCC) is directly proportional to the concentration and content of cellulose (Kanbayashi and Miyafuji 2016; Yang *et al.* 2021a, 2022a,b,c). Meanwhile, fluorescence microscopy can be utilized to evaluate lignin distribution and content in wood cells through the green fluorescence brightness of lignin (GFBL). Higher GFBL indicate greater concentration and content of lignin (Kanbayashi 2016; Liu *et al.* 2017; Kiyoto *et al.* 2018; Yang *et al.* 2021a, 2022a,b,c). This technique requires only a limited quantity of samples from wooden components, while avoiding noticeable damage. Consequently, it is increasingly utilized for evaluating the material health status of wooden components in ancient buildings.

In this study, various microscopic observation techniques, including bright-field light, polarized light, and fluorescence methods, were utilized to analyze the extent of cell wall damage as well as the distribution and content of cellulose and lignin in the wooden components of Tingbao Yang's former residence. Additionally, decay levels would be categorized based on cellulose and lignin content. Furthermore, an extensive analysis of decay causes was conducted by examining internal characteristics exhibited by different wood species alongside external conditions. The objective of this research was to establish a foundation for scientifically selecting subsequent conservation strategies.

EXPERIMENTAL

Materials

Sixty-one samples were randomly collected from various wooden components, including columns, beams, lintels, purlins, rafters, and other wooden components in Rooms 1 to 23 of Tingbao Yang's former residence (Fig. 1) located in Jiefang Road, Wancheng District, Nanyang City, Henan Province. The sampling was conducted using an increment borer (10-100-1027, Haglöf AB, Mora, Sweden). The samples consisted of visually decayed wood as well as moth-eaten and undamaged wood. Control samples were obtained from normal positions within these wooden components. Table 1 provides specific details

on the sampling locations and the names of the wood species.

Fig. 1. Present state of Yang Tingbao's former residence

Table 1. Material Sampling Data

Room No.	Sample No.	Sampling Position of the Samples	Wood Species Identification (Yang *et al*. 2024)
Room 2	No. 1	left front eave column in the secondary room on left	*P. bungeana*
	No. 2	left front golden column in the secondary room on left	*P. tomentosa*
	No. 3	left front eave column in the bright room	*U. pumila*
	No. 10	right front eave column in the secondary room on right	*U. pumila*
	No. 11	right front golden column in the secondary room on the right	*P. tomentosa*
	No. 12	right front golden column in the bright room	*P. tomentosa*
	No. 14	right rear golden column in the bright room	*P. brachytyla*
	No. 15	left front golden column in the bright room	*P. tomentosa*
	No. 40	penetrating tie in the secondary room on the left	*C. lanceolata*
	No. 41	left five-beam in the secondary room on the left.	*P. sinensis*
	No. 42	front melon column beneath the left three-beam in the secondary room on the left	*L. potaninii* var. *australis*
	No. 43	rear eave rafter	*C. lanceolata*
	No. 44	rear eave Lintel	*P. bungeana*
	No. 46	front eave purlin	*C. lanceolata*

	No. 47	rear eave Lintel	*L. potaninii* var. *australis*
	No. 48	baotou beam in the secondary room on the left	*P. tomentosa*
Room 3	No. 6	left front golden column in the bright room	*U. pumila*
	No. 7	right front golden column in the bright room	*U. pumila*
	No. 8	right front eave column in the bright room	*C. lanceolata*
	No. 9	left front eave column in the bright room	*U. pumila*
	No. 49	left five-beam in the bright room	*U. pumila*
	No. 50	rear melon column beneath the left three-beam in the bright room	*U. pumila*
Room 4	No. 4	left front golden column in the bright room	*U. pumila*
	No. 5	right front golden column in the bright room	*U. pumila*
	No. 51	the left five-beam in the bright room	*U. pumila*
	No. 52	the rear melon column above the left five-beam in the bright room	*U. pumila*
	No. 54	the front eave purlin in the end room on the right	*C. lanceolata*
	No. 55	the front eave lintel in the end room on the right	*C. lanceolata*
Room 5	No. 16	left rear golden column in the bright room	*P. sinensis*
	No. 17	right rear golden column in the bright room	*P. sinensis*
	No. 18	right front eave column in the bright room	*P. sinensis*
	No. 19	left front eave column in the bright room	*P. sinensis*
	No. 20	left front eave column in the secondary room on left	*P. sinensis*
	No. 21	right front eave column in the secondary room on right	*P. sinensis*
	No. 22	lintel beneath the left five-beam in the bright room	*U. pumila*
	No. 23	the left five-beam in the bright room	*U. pumila*
	No. 24	rear melon column above the left five beam in the bright room	*U. pumila*
	No. 25	left rear one step beam in the bright room	*U. pumila*
	No. 26	rear melon column beneath the left three-beam in the bright room	*U. pumila*
	No. 27	front eave purlin in the end room on the right	*C. lanceolata*
	No. 28	front eave lintel in the end room on the right	*P. sinensis*
	No. 29	front eave rafter	*C. lanceolata*
Room 6	No. 34	left five-beam in the bright room	*U. pumila*
	No. 35	rear eave purlin in the bright room	*C. lanceolata*
	No. 36	rear melon column above the left five-beam in the bright room	*C. lanceolata*
	No. 37	rear melon column beneath the left three-beam in the bright room	*U. pumila*
	No. 38	End of front eave flying rafter	*L. potaninii* var. *australis*
	No. 39	front eave purlin in the bright room	*C. lanceolata*
	No. 45	eave rafter in the auricular chamber on the left	*C. lanceolata*
Room 7	No. 30	right five-beam in the bright room.	*U. pumila*
	No. 31	front melon column above the right five-beam in the bright room	*U. pumila*
	No. 32	rear eave rafter in the bright room	*C. lanceolata*
	No. 33	front eave purlin in the bright room	*C. lanceolata*
Room 11	No. 56	left rear eave column in the bright room	*C. lanceolata*
	No. 57	right rear eave column in the bright room	*C. lanceolata*
Room 17	No. 58	left rear golden column in secondary room on the left	*C. lanceolata*
	No. 59	right front golden column in the bright room	*P. massoniana*
Room 18	No. 60	front eave flying rafter	*P. massoniana*
Room 21	No. 63	right five-beam in the bright room	*U. pumila*
	No. 64	rear eave rafter	*C. lanceolata*
Room 22	No. 62	right five-beam in the bright room	*C. lanceolata*

The predominant wood species identified by the authors (Yang *et al*. 2024) include larch (*Larix potaninii* var. *australis*), spruce (*Picea brachytyla*), lace-bark pine (*Pinus bungeana*), Masson pine (*Pinus massoniana*), Chinese Douglas fir (*Pseudotsuga sinensis*), Chinese fir (*Cunninghamia lanceolata*), poplar (*Populus tomentosa*), and elm (*Ulmus pumila*).

METHODS

Pretreatment of Wooden Component Samples

Some samples were seriously damaged by decay fungi, such that the material had become soft. In order to increase the strength of the samples and facilitate better sectioning, all the samples were embedded with polyethylene glycol (PEG). The processing procedures for wooden components were conducted in accordance with the following steps (Yang *et al.* 2021a, 2022a,b,c): (1) Air evacuation: The small samples were placed in a vacuum dryer to eliminate air from within the wood samples. (2) Infiltration with PEG (molecular weight = 2000): The sample was sequentially immersed in aqueous solutions of PEG at concentrations of 20%, 40%, 60%, and 80% before finally being subjected to a concentration of 100%. Each gradient underwent a processing duration of 48 h at a temperature of 60 °C, with two infiltrations utilizing the 100% PEG solution. (3) Embedding in PEG: The samples were positioned at the base of an embedding mold and subsequently covered with an aqueous solution of 100% PEG. A plastic embedding box was then employed to enclose the setup. (4) Freezing: The embedding box was placed inside a freezer for approximately 10 min.

Sectioning of Wooden Component Samples

The sections were prepared following the steps outlined in GB/T 29894 (2013) and Yang *et al.* (2021a, 2022a,b,c). (1) Firstly, the embedded samples were carefully sectioned using a microtome (HistoCore AUTOCUT, Leica Biosystems, Wetzlar, Germany) to obtain transverse, radial, and tangential sections with a thickness of approximately 10 μm. (2) Subsequently, the sections were subjected to baking at 60 °C for about 60 min to eliminate excess water and prevent curling. (3) Dehydration was then performed by immersing the slices sequentially in ethanol solutions of increasing concentrations (50%, 75%, 95%, and finally 100%), each treatment lasted for a duration of 10 min. (4) To remove any remaining fat content from the slices, they were defatted using dimethyl benzene solution for a period of 3 min. (5) Finally, neutral gum was applied as a sealing agent after all treatments. It is important to note that no red O dye was used on any of the slices to avoid interference with polarized light and fluorescence observations.

Microscopic Observation under Bright-field Light, Polarized Light, and Fluorescence

A polarizing microscope can convert ordinary light into polarized light, so as to analyze the birefringence of crystals. The crystalline region of cellulose in wood cell wall has birefringence, so the cellulose concentration can be determined according to the intensity of birefringence, so as to qualitatively assess the degradation of wood cellulose (Cui *et al*. 2016). Filter blocks with different wavelengths of fluorescence microscope can stimulate the fluorescent material in wood to emit fluorescence of different colors. Lignin in wood cell wall can produce green fluorescence when irradiated by blue filter block.

Therefore, the lignin concentration can be determined according to the intensity of green fluorescence, and the degradation of wood lignin can be qualitatively assessed (Cui *et al*. 2016). The microstructures of the prepared slices were observed using bright-field light, polarized light, and fluorescence under a standing fluorescence microscope (ECLIPSE Ni-U, Nikon, Tokyo, Japan). The degree of cell damage was assessed through bright-field observation. The qualitative measurement of cellulose crystal distribution and content in the cell wall was conducted using polarizing light. Higher birefringence values indicate higher concentrations and contents of cellulose. The qualitative measurement of lignin distribution and content in the cell wall was performed using fluorescence (Blue Monochromatic filter block: excitation wavelength 450 to 490 nm; Block 510 nm; emission wavelengths: 515 nm). Higher brightness levels of green fluorescence and red fluorescence correspond to higher concentrations and contents of lignin (Yang *et al*. 2021a, 2022a,b,c).

Wood degradation level was determined based on the BBCC as well as the GFBL. If these values are similar to those of the control wood, then it is defined as slight decay; If they decrease by 1/3 to 1/2 compared to the control, then it is defined as medium decay; If they decrease by more than 1/2 compared to the control, then it is defined as serious decay.

RESULTS AND DISCUSSION

Decay Levels of Larch Wooden Components

Figure 2 illustrates the microstructure of polarization and fluorescence effects in larch wooden components, along with their corresponding control wood.

Number of Wooden Components	Bright-field light, 40x	Polarized light, 40x	Green fluorescence, 40x	Decay levels
No. 38	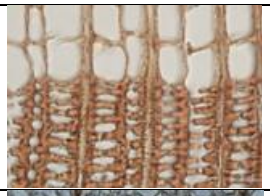	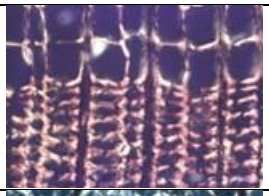	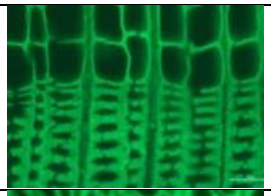	Severe decay
No. 42	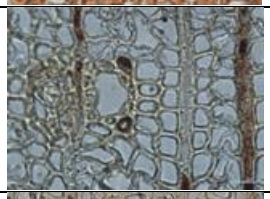		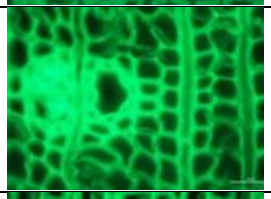	Moderate decay
No. 47	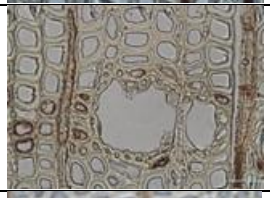		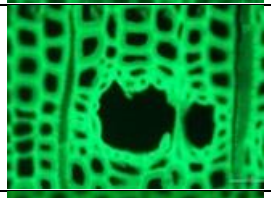	Slight decay
Control		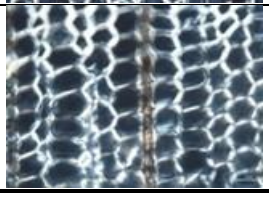	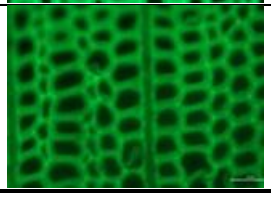	Healthy

Fig. 2. Microstructure of polarization and fluorescence effects in larch wooden components

It is noteworthy that tracheids in Nos. 42 and 47 remained predominantly intact, while those in No. 38 exhibited evident structural damage when examined under bright-field light. Under polarized light, the BBCC of tracheids in Nos. 42 and 47 exhibited a noticeable presence, a little weaker compared to the control wood. Notably, there was an evident decrease in the BBCC within the middle layer (S_2) and inner layer (S_3) of tracheid in No. 47, indicating that a certain level of degradation had occurred. Moreover, tracheid in No. 38 displayed a greater reduction in the BBCC, suggesting a higher degree of cellulose degradation. Under fluorescence, the GFBL of tracheids in Nos. 42 and 47 exhibited noticeable intensity, suggesting that the lignin within these two wooden components remained intact or only slightly damaged by wood decay fungi. However, an evident reduction was observed in No. 38, particularly within the compound middle lamellas (CML) and cell corners (CC), indicating a more extensive degradation of lignin. Based on comprehensive analysis, it can be concluded that No. 47 exhibited slight decay, No. 42 displayed moderate decay, while No. 38 demonstrated severe decay.

Decay Levels of Spruce Wooden Components

Figure 3 illustrates the microstructure of polarization and fluorescence effects in spruce wooden component and its control wood. A comparative analysis reveals that the tracheids in No. 14 exhibited a higher incidence of perforations when observed under bright-field light, indicating more severe damage to its structural integrity compared to the control wood. Furthermore, examination through a polarizing microscope demonstrated an evident reduction in the BBCC of tracheids as opposed to the control wood, suggesting a greater extent of degradation in cellulose arrangement. Under fluorescence observation, there was slight attenuation of the GFBL of tracheids compared to the control wood, indicating a certain degree of lignin degradation. Based on analysis, it can be concluded that No. 14 exhibited severe decay.

Number of Wooden Components	Bright-field light, 40x	Polarized light, 40x	Green fluorescence, 40x	Decay levels
No. 14		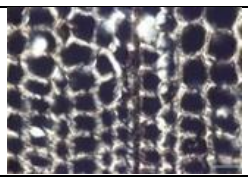	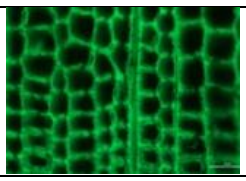	Severe decay
Control			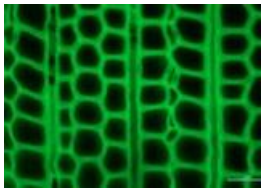	Healthy

Fig. 3. Microstructure of polarization and fluorescence effects in spruce wooden components

Decay Levels of Lace-bark Pine Wooden Components

Figure 4 illustrates the microstructure of polarization and fluorescence effects in lace-bark pine wooden components. Under bright-field light, the tracheids in Nos. 1 and 44 remained predominantly intact. However, under polarized light, there was a significant weakening of the BBCC of the tracheids, accompanied by a loosening of the overall

arrangement of crystalline cellulose. This observation suggests that these two wooden components had undergone a higher degree of cellulose degradation. Furthermore, fluorescence analysis revealed a noticeable reduction in the GFBL of tracheids, indicating more extensive lignin degradation. Based on the analysis, it can be concluded that Nos. 1 and 44 exhibited severe decay.

Number of wooden components	Bright-field light, 40x	Polarized light, 40x	Green fluorescence, 40x	Decay levels
Nos. 1 and 44	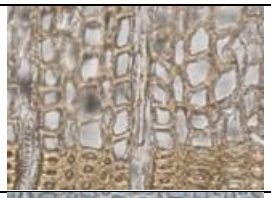		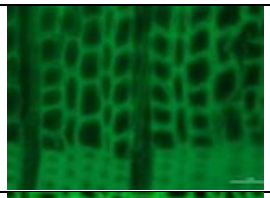	Severe decay
Control		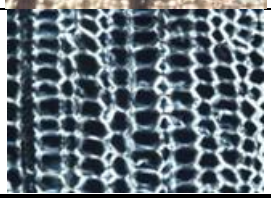	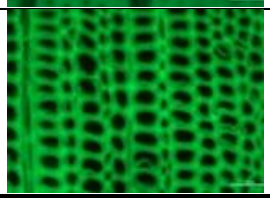	Healthy

Fig. 4. Microstructure of polarization and fluorescence effects in lace-bark pine wooden components

Number of wooden components	Bright-field light, 40x	Polarized light, 40x	Green fluorescence, 40x	Decay levels
No. 59	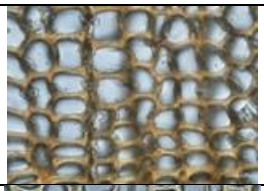		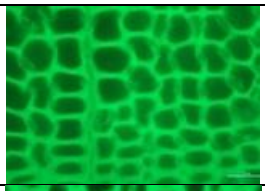	Severe decay
No. 60	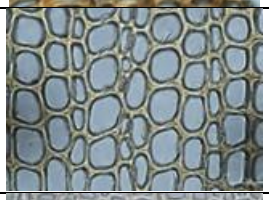	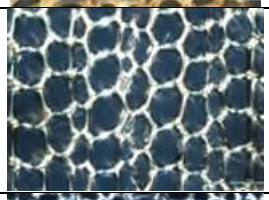	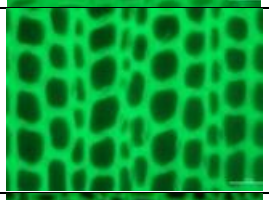	Slight decay
Control	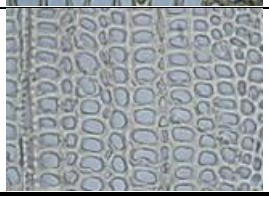	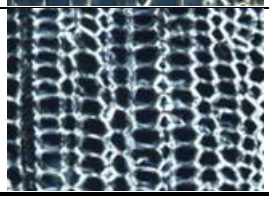	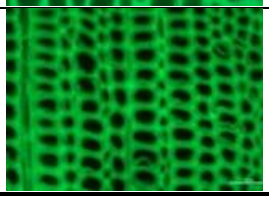	Healthy

Fig. 5. Microstructure of polarization and fluorescence effects in Masson pine wooden components

Decay Levels of Masson Pine Wooden Components

Figure 5 illustrates the microstructure of polarization and fluorescence effects in Masson pine wooden components along with the control wood. Under bright-field light, the tracheids in Nos. 59 and 60 appeared predominantly intact. However, when examined using a polarizing microscope, the BBCC of tracheids in No. 60 was generally weaker compared to that of the control wood, indicating a slight degradation of cellulose in No.

60. Conversely, the tracheids in No. 59 exhibited a yellowish BBCC with minimal intensity, indicating a greater degree of degradation of cellulose in No. 59. Fluorescence microscopy revealed that a GFBL of the tracheids in both Nos. 59 and 60 was similar to that in the control wood. Based on comprehensive analysis, it can be concluded that No. 59 exhibited severe decay while No. 60 showed slight decay.

Decay Levels of Chinese Douglas Fir Wooden Components

Figure 6 illustrates the microstructure of polarization and fluorescence effects in Chinese Douglas fir wooden components. The tracheids in all samples remained predominantly intact structures when observed under bright-field light. However, examination through a polarizing microscope revealed an evident reduction of the BBCC of tracheids in Nos. 17 to 21 and 28, indicating noticeable degradation of cellulose. Additionally, there was a noticeable decrease in the BBCC of tracheids No.16, suggesting partial degradation caused by decaying bacteria activity. Furthermore, No. 41 exhibited observable BBCC, implying slight degradation. Under fluorescence, the GFBL of tracheids in all samples remained relatively prominent. However, there was a noticeable reduction in GFBL in the CML and CC of tracheid in No. 41. This observation suggests that there has been some degradation of lignin in No. 41. Based on analysis, it can be concluded that Nos. 17 to 21 and 28 exhibited severe decay, while No. 16 showed moderate decay and No. 41 exhibited slight decay.

Number of wooden components	Bright-field light, 40x	Polarized light, 40x	Green fluorescence, 40x	Decay levels
Nos. 17-21 and 28			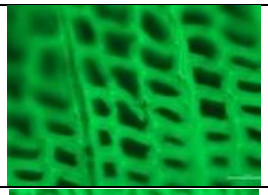	Severe decay
No. 16			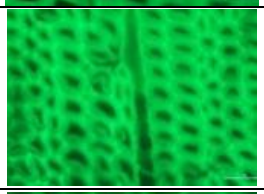	Moderate decay
No. 41			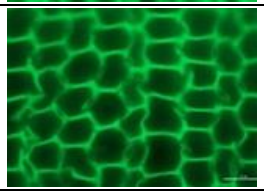	Slight decay
Control		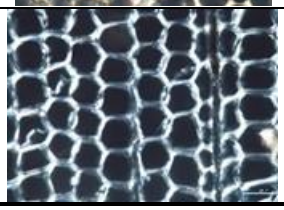	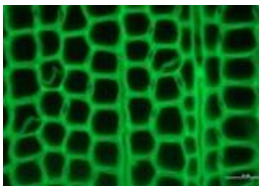	Healthy

Fig. 6. Microstructure of polarization and fluorescence effects in Chinese Douglas fir wooden components

Decay Levels of Chinese Fir Wooden Components

Figure 7 illustrates the microstructure of polarization and fluorescence effects in Chinese fir wooden components, along with their corresponding control wood. Upon comparison with the control wood, it is evident that the tracheids in all wooden components remained predominantly intact. Under polarized microscopy, a near-complete loss of the BBCC was observed in tracheids of Nos. 32, 35, and 54 to 55 compared to the control wood, indicating a nearly complete degradation of cellulose. Tracheids in Nos. 8, 27, 29, 39, and 40, as well as Nos. 43, 45, 57, and 58 exhibited a noticeable decrease in BBCC, suggesting an evident degradation of cellulose. Although there was observable BBCC of tracheids in Nos. 33, 36, 46, 56, and 64, it was obviously weaker than that observed in the control wood, suggesting a certain degree of cellulose degradation. The GFBL of tracheids in all wooden components were clearly similar to that of the control wood under fluorescence microscopy, indicating that the lignin in these wooden components remained intact or experienced minimal damage from wood decay fungi. Based on analysis, it can be inferred that Nos. 32, 35, and Nos. 54 and 55 exhibited severe decay, while Nos. 8, 27, 29, 39 and 40, 43, 45, 57 and 58 and 62 showed moderate decay and Nos. 33, 36, 46, 56, and 64 displayed slight decay.

Number of wooden components	Bright-field light, 40x	Polarized light, 40x	Green fluorescence, 40x	Decay levels
Nos. 32, 35, 54 and 55			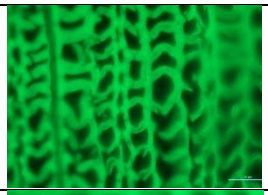	Severe decay
Nos. 8, 27, 29, 39 and 40, 43, 45, 57 and 58, 62			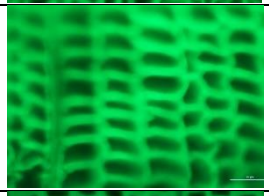	Moderate decay
Nos. 33, 36, 46, 56, 64		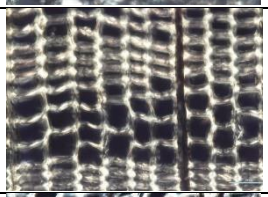	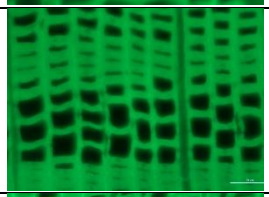	Slight decay
Control		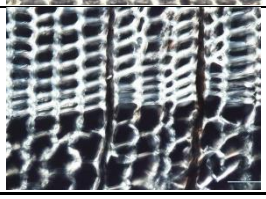	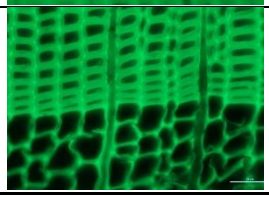	Healthy

Fig. 7. Microstructure of polarization and fluorescence effects in Chinese fir wooden components

Decay Levels of Poplar Wooden Components

Figure 8 illustrates the microstructure of polarization and fluorescence effects in poplar wooden components, along with their corresponding control wood specimens. Notably, Nos. 2 and 11 to 12 exhibited intact structures in wood fibers; however, Nos. 15 and 48 displayed severe damage under bright-field light. Polarized microscopy revealed

that the BBCC of vessels and wood fibers in No. 12 were similar to that of the control wood. Vessels and wood fibers in Nos. 2 and 11 showed a weaker BBCC compared to the control, suggesting a certain degree of degradation of cellulose. Furthermore, a greater reduction in BBCC was observed in Nos. 15 and 48, indicating a higher level of cellulose degradation. Under the fluorescence microscope, it was observed that the GFBL of vessels and wood fibers in No. 12 were similar to that in the control wood. Notably, visible GFBL were detected in Nos. 2 and 11. There was a noticeable GFBL in the CML and CC of vessels and wood fibers in samples No. 15 and No. 48; however, none were observed in the S_2. Based on analysis, it can be concluded that Nos. 15 and 48 exhibited severe decay, Nos. 2 and 11 showed moderate decay, while No. 12 displayed slight decay.

Number of wooden components	Bright-field light, 40x	Polarized light, 40x	Green fluorescence, 40x	Decay levels
Nos. 15 and 48	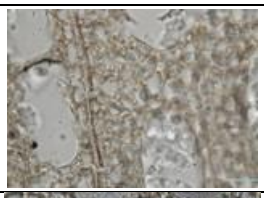		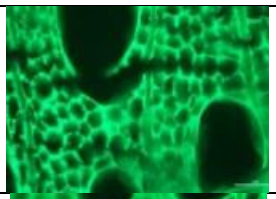	Severe decay
Nos. 2 and 11			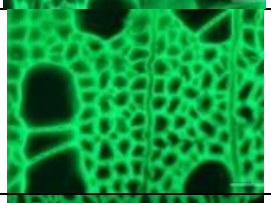	Moderate decay
No. 12	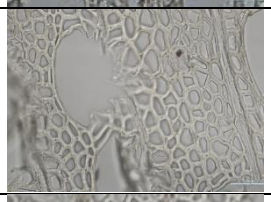	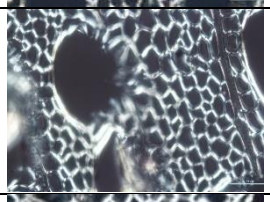	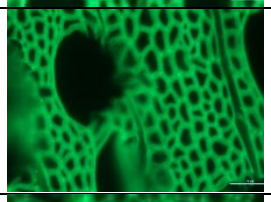	Slight decay
Control	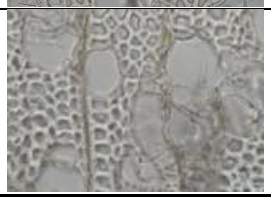	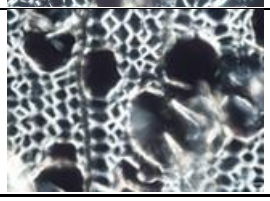	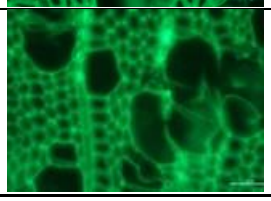	Healthy

Fig. 8. Microstructure of polarization and fluorescence effects in poplar wooden components

Decay Levels of Elm Wooden Components

Figure 9 illustrates the microstructure of polarization and fluorescence effects in elm wooden components, along with the control wood. When observed under bright-field light, the majority of samples displayed that the vessels and wood fibers were essentially intact, except for Nos. 4, 6, 10, 34, and No. 63, which displayed noticeable deformation. Under polarizing microscope observation, the BBCC of vessels and wood fibers in Nos. 3, 5, 7, 30, and Nos. 49 to 51 were similar to that observed in control wood, indicating no obvious cellulose consumption by decay fungi. However, an obviously weaker BBCC was observed in Nos. 4, 9, 22, 23, 24, 26, 31, 37, 52, and 63. In contrast to this finding, Nos. 6, 10, 25, and 34 exhibited a greater weakness in BBCC with thinner cell walls of vessels and wood fibers, this result indicates a more extensive degradation process had occurred in these samples. Under the fluorescence microscope, with the exception of Nos. 6, 10, 25,

and 34, the GFBL of vessels and wood fibers in samples were prominently evident. This observation suggests that there was no excessive consumption of lignin by wood decay fungi. Based on analysis, it can be concluded that Nos. 6, 10, 25, and 34 exhibited severe decay, Nos. 4, 9, 22 to 24, 26, 31, 37, 52, and 63 showed moderate decay, while Nos. 3, 5, 7, 30, and 49 to 51 displayed slight decay.

Number of wooden components	Bright-field light, 40x	Polarized light, 40x	Green fluorescence, 40x	Decay levels
Nos. 6, 10, 25, and 34	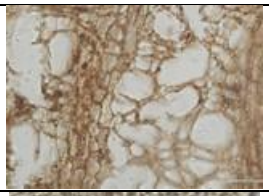		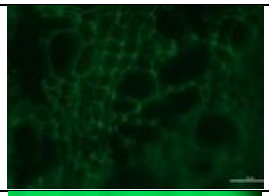	Severe decay
Nos. 4, 9, 22 to 24, 26, 31, 37, 52, and 63				Moderate decay
Nos. 3, 5, 7, 30, and 49 to 51	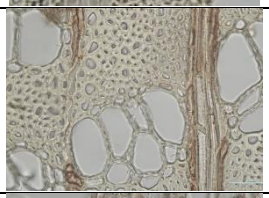	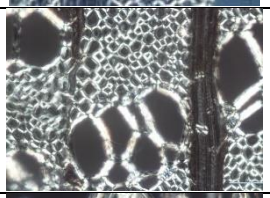	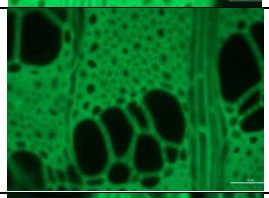	Slight decay
Control		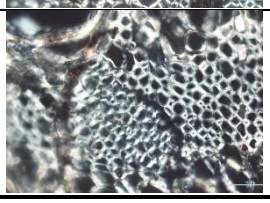	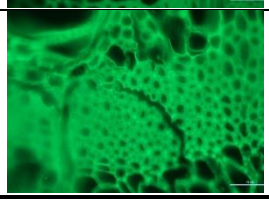	Healthy

Fig. 9. Microstructure of polarization and fluorescence effects in wooden components of elm

Factors Contributing to the Deterioration of Wooden Components

Generally, wood decay requires the simultaneous presence of five conditions: (1) abundant nutrients; (2) elevated moisture content (MC ≥ 26%); (3) optimal temperature range (25 ℃ to 40 ℃); (4) acidic environment (pH 4.0 to 6.5); and (5) sufficient oxygen levels (1.5 to 10 mmHg) (Guo *et al.* 2010). Among these factors, the internal moisture content of wood is directly influenced by external environmental conditions, such as temperature, humidity, and rainfall, which are considered extrinsic factors. In contrast, the type and concentration of nutrients as well as the pH value of the medium are associated with intrinsic properties of wood.

Differences in Natural Durability of Wood Species Used for Wooden Components

From the difference of natural durability of the wood species, larch demonstrates a moderate level of resistance against rot but exhibits weak resistance against insects and ants (Cheng *et al.* 1992; Ma *et al.* 2011). Spruce also displays weak rot resistance and is susceptible to damage from insects and ants. Lace-bark pine show a lack of decay resistance and is vulnerable to attacks from ants and marine wood-boring organisms.

Masson pine typically has a wide sapwood-to-heartwood ratio, resulting in low decay resistance, high susceptibility to termite infestation, vulnerability to harm from marine wood-boring organisms, and an increased likelihood of damage. Chinese Douglas fir possesses medium durability with challenges in anti-corrosion treatment. Chinese fir exhibits low resistance to rot, with the sapwood being highly susceptible to termite attacks. Elm and poplar both exhibit weak resistance against ants; however, elm shows slight resilience against decay, whereas poplar trees are particularly prone to heartwood decay during their growth. Moreover, the pH value of these woods is between 4.0 to 6.5, which provides indispensable conditions for its decay (Cheng *et al.* 1992; Ma *et al.* 2011).

Based on the research findings of Guo *et al.* (2010), soft rot fungi consume both cellulose and hemicellulose of wet wood, as well as lignin, while brown rot fungi primarily consume cellulose but retain a noticeable amount of lignin of half wet wood. The authors in this paper analyzed the polarizing light and fluorescence effects of some wood species in Xichuan hall (Yang *et al*. 2022a), Chikan ancient town (Yang *et al*. 2022b), and Danxia temple (Yang *et al.* 2022c), and found that *Schima* spp. suffered from the damage of white rot fungi, *C. lanceolata* suffered from the damage of soft rot fungi, *Quercus rubra, Betula albosinensis*, and *Pterocarya stenoptera* suffered from the damage of brown rot fungi. Combined with analysis utilizing polarizing light and fluorescence effects in this paper, it can be speculated that the wooden components of larch, spruce, white bark pine, and poplar are susceptible to varying degrees of damage from soft rot fungi. Similarly, the wooden components of Masson pine, Chinese Douglas fir, Chinese fir, and elm exhibit distinct levels of damage caused by brown rot fungi.

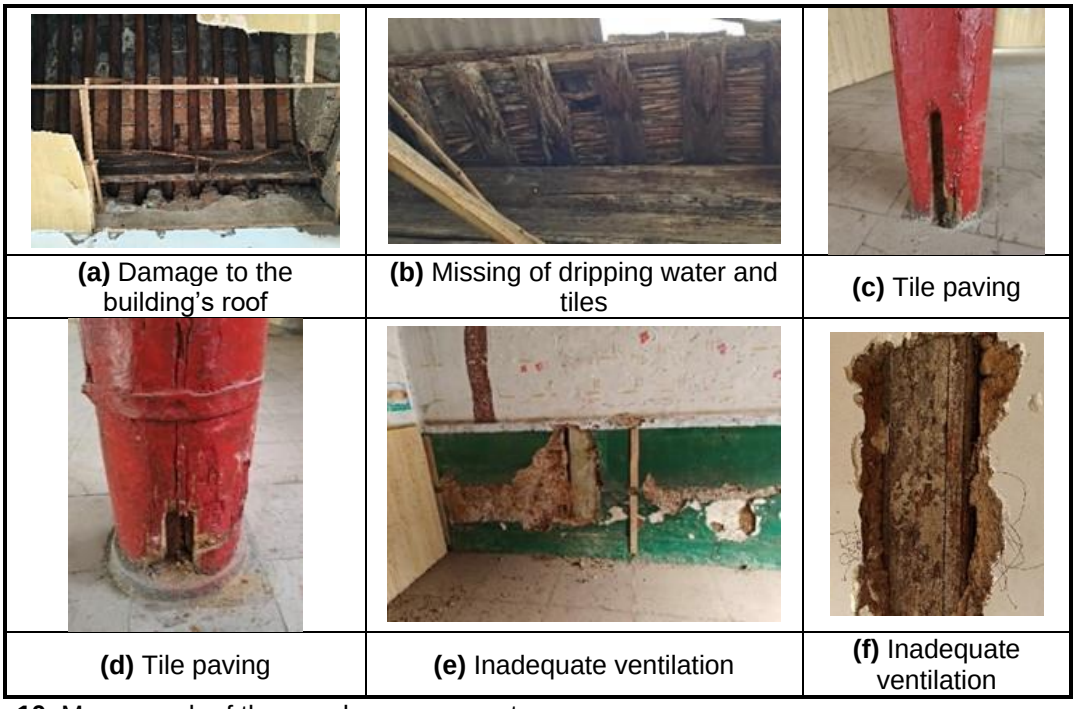

Fig. 10. Macrograph of the wooden components

Influence of External Factors on the Wooden Components

External factors directly impact the fluctuation in internal MC of wooden components. Dry or water-saturated wood rarely experiences instances of wood decay (Martín and López 2023). Once the MC of wood exceeds the fiber saturation point (F.S.P.<

26%), it becomes vulnerable to microbial and insect infestation, with higher MC resulting in more severe decay (Martín and López 2023; Guo *et al.* 2010). Based on the authors' analysis, several external factors were identified that contributed to the deterioration of the wooden components in Tingbao Yang's former residence as follows: Firstly, extensive damage to the building's roof (Fig. 10a) and missing part of dripping water and tiles (Fig. 10b) result in rainwater infiltration into beam frames, purlins, and rafters, consequently, leading to an increase in internal MC within these wooden elements. Secondly, the elevation of indoor and outdoor ground levels in certain rooms, combined with contemporary paving for specific indoor tiles (Fig. 10c to d), exacerbates vulnerability to column root intrusion caused by condensed water on the surface of stone foundations. Additionally, inadequate ventilation due to wooden components being enclosed within walls or wooden blocks (Fig. 10e to f) amplifies the likelihood of decay manifestation.

CONCLUSIONS

Polarization and fluorescence analyses were performed on the wooden components in Tingbao Yang's former residence, along with investigations into the causes of decay. Based on these comprehensive studies, the following conclusions can be drawn.

1. The analysis of polarization and fluorescence effects reveals that there are varying degrees of decay in the wooden components of larch, spruce, white bark pine, Masson pine, Chinese Douglas fir, Chinese fir, poplar, and elm.
2. The primary internal cause contributing to the decay of these wooden components is the inherent low natural durability of the wood species themselves and external factors, such as damaged roofs, missing dripping water and tiles, uneven indoor and outdoor ground levels, modern tile paving indoors, and inadequate ventilation.
3. Based on an analysis of the degree of decay and causes affecting the wooden components, several conservation strategies have been proposed: For slightly or non-temporarily decayed wooden components, it is recommended to perform anti-decay treatment, while chemical reinforcement treatment should be employed for moderately or severely decayed ones; It is crucial to promptly restore the damaged roof to its original condition, and the missing dripping water and tiles should be replaced without delay; Restoration work is necessary for part of the indoor floor that has been elevated and replaced with contemporary tiles in accordance with its original shape. Additionally, it is imperative to apply waterproof treatment to prevent capillary water absorption at the base of the columns; Considering the potential accumulation of moisture within walls or wooden blocks, it is crucial to promptly implement ventilation measures for the wooden columns to mitigate any potential damage caused by excessive internal moisture content.

ACKNOWLEDGMENT

Yan Yang and Haidi Ji contributed equally in this work. This study was financially supported by the Key Research and Development and Promotion Project of Henan Province (242102320293), and Key Research Project of University in Henan Province (24A560017).

REFERENCES CITED

Bari, E., Daniel, G., Yilgor, N., Kim, J.-S., Tajick-Ghanbary, M.-A., Singh, A.-P., and Ribera, J. (2020). "Comparison of the decay behavior of two white-rot fungi in relation to wood type and exposure conditions," *Microorganisms* 8(12), article 1931. DOI: 10.3390/microorganisms8121931

Bari, E., Daryaei, M.-G., Karim, M., Bahmani, M., Schmidt, O., Woodward, S., Ghanbary, M.-A.-T., and Sistani, A. (2019). "Decay of *Carpinus betulus* wood by *Trametes versicolor* – An anatomical and chemical study," *International Biodeterioration and Biodegradation* 137, 68-77. DOI: 10.1016/j.ibiod.2018.11.011

Bari, E., Daryaei, M.-G., Karim, M., Bahmani, M., Schmidt, O., Woodward, S., Ghanbary, M.-A.-T., and Sistani, A. (2019). "Decay of *Carpinus betulus* wood by *Trametes versicolor* – An anatomical and chemical study," *International Biodeterioration and Biodegradation* 137, 68-77. DOI: 10.1016/j.ibiod.2018.11.011

Brischke, C., Stricker, S., Meyer-Veltrup, L., and Emmerich, L. (2019). "Changes in sorption and electrical properties of wood caused by fungal decay," *Holzforschung* 73(5), 445-455. DOI: 10.1515/hf-2018-0171

Broda, M., Popescu, C.-M., Curling, S.-F., Timpu, D.-I., and Ormondroyd, G.-A. (2022). "Effects of biological and chemical degradation on the properties of Scots pine wood—Part I: Chemical composition and microstructure of the cell wall," *Materials* 15(07), article 2348. DOI: 10.3390/ma15072348

Cavallaro, D., Lucejko, J.-J., Pizzo, B., Mohammed, M.-Y., and Sloggett, R. (2017). "A critical evaluation of the degradation state of dry archaeological wood from Egypt by SEM, ATR-FTIR, wet chemical analysis and Py (HMDS)-GC-MS," *Polymer Degradation and Stability* 146, 140-154. DOI: 10.1016/j.polymdegradstab.2017.10.009

Chang, L.-H., Dai, J., and Qian, W. (2016). "Nondestructive testing of internal defect of ancient architecture wood members based on Shapley value," *Journal of Beijing University of Technology* 42(6), 886-892. DOI: 10.11936/bjutxb2015110081

Chen, Y., Chen, L., and Dai, S.-B. (2018). "Study of anti-corrosion measures for wooden pillars of historical architectures," *Sciences of Conservation and Archaeology* 30(1), 63-71. DOI: 1005-1538(2018)01-0063-09

Cheng, J. Q., Yang, J. J., and Liu, P. (1992). *Atlas of Chinese Woods*, China Forestry Publishing House, Beijing, China.

Cui, X.-J., Qiu, J., and Gao, J.-R. (2016). "Evaluation of the decay level and reinforcement of ancient wood by fluorescence and polarizing technology," *Sciences of Conservation and Archaeology* 28(4),48-53. DOI: 1005-1538(2016)04-0048-06

Dai, J., Chang, L.-H., Qian, W., and Chang, H. (2017). "A study on the non-destructive method of testing internal and external defects of wooden components of historical buildings," *Architectural Journal* 2017(02), 7-10.

Dong, S.-H., Wang, C., Xiang, J.-K., and Zhang, G. (2020). "Research on changes of chemical composition and structure of the minor carpentry work in Gongshu Hall of Hu County based on FTIR—ATR," *Infrared* 41(7), 30-37. DOI: 10.3969/j.issn.1672-8785.2020.07.006

GB/T 29894 (2013). "General method of wood identification," Standardization Administration of China, Beijing, China.

Guo, M.-L., Lan, H.-F., and Qiu, J. (2010). *Wood Deterioration and Preservation*, China Metrology Publishing House, Beijing, China.

Kanbayashi, T., and Miyafuji, H. (2016). "Effect of ionic liquid treatment on the ultrastructural and topochemical features of compression wood in Japanese cedar (*Cryptomeria japonica*)," *Scientific Reports* 6, article 30147. DOI: 10.1038/srep30147.

Kiyoto, S., Yoshinaga, A., Fernandez-Tendero, E., Day, A., Chabbert, B., and Takabe, K. (2018). "Distribution of lignin, hemicellulose, and arabinogalactan protein in hemp phloem fibers," *Microscopical Society of Canada* 24(4), 442-452. DOI: 10.1017/S1431927618012448

Liu, C.-W., Su, M.-L., Zhou, X.-W., Zhao, R.-J., Lu, J.-X., and Wang, Y.-R. (2017). "Analysis of content and distribution of lignin in cell wall of transgenic poplar with Fourier infrared spectrum (FTIR) and confocal laser scanning microscopy (CLSM)," *Spectroscopy and Spectral Analysis* 37(11), 3404-3408. DOI: 10.3964/j.issn.1000-0593(2017)11-3404-05

Ma, X.-X., Jiang, M.-L., and Li, Z.-Q. (2011). *Wood Biodegradation and Protection*, China Forestry Publishing House, Beijing, China.

Martín, J.-A., and López, R. (2023). "Biological deterioration and natural durability of wood in Europe," *Forests*. 14, article 283. DOI: 10.3390/f14020283

Tamburini, D., Lucejko, J.-J., Pizzo, B., Mohammed, M.-Y., and Sloggett, R. (2017). "A critical evaluation of the degradation state of dry archaeological wood from Egypt by SEM ATR-FTIR wet chemical analysis and Py (HMDS)-GC-MS," *Polymer Degradation and Stability* 146, 140-154. DOI: 10.1016/j.polymdegradstab.2017.10.009

Ueda, R., Sawata, K., Takanashi, R., Sasaki, Y., and Sasaki, T. (2020). "Degradation of shear performance of screwed joints caused by wood decay," *Journal of Wood Science* 66(1), 1-11. DOI: 10.1186/s10086-020-01889-w

Yang, Y., Sun, H., Li, B., Wang, A.-F., Zhao, R., Wang, W., He, Y.-M., Yang, S., Han, Y.-X., and Sun, W.-Y. (2020). "FTIR spectroscopy analysis of the changes in chemical composition of wooden components in the ancient building of Xichuan Guild Hall," *Forest Products Journal* 70(4), 448-452. DOI: 10.13073-FPJ-D-20-00028

Yang, Y., Sun, H., Yang, S., Wang, A.-F., Zhao, R., Wang, W., He, Y.-M., Li, B., Zhang, B.-X., and Wu, Q. (2021a). "Internal cause analysis of damage of wooden components in Danxia temple ancient architectures: Tree species," *Wood Research* 66(2), 297-308. DOI: 10.37763/wr.1336-4561/66.2.297308

Yang, Y., Sun, H., Yang, S., Sun, W.-Y., Zhao, Y., Li, B., Wang, W., Zhang, X.-Q., Jiang, S.-L., and Xu, Q. (2021b). "Fourier-transform infrared spectroscopy analysis of the changes in chemical composition of wooden components: Part II—The ancient building of Danxia Temple," *Forest Products Journal* 71(3), 283-289. DOI: 10.13073/FPJ-D-21-00015

Yang, Y., Sun, H., Li, B., Han, L., Wang, A.-F., Wang, W., He, Y.-M., and Zhao, R. (2022a). "Study on the identification and the extent of decay of the wooden components in the Xichuan Guild Hall ancient architectures," *International Journal*

of Architectural Heritage 16(3), 405-414. DOI: 10.1080/15583058.2020.1786190

Yang, Y., Zhang, X.-Q., Xu, Q., Wang, P.-Y., Jiang, S.-L., Min, Y., Sun, W.-Y., Li, B., Fan, Y.-L., and Yang, S. (2022b). "Evaluation of the decay levels of wooden components in arcade buildings in the ancient town Chikan *via* polarized light fluorescence and FTIR Spectra," *Wood Research* 67(4), 545-557. DOI: 10.37763/wr.1336-4561/67.4.545557

Yang, Y., Li, B., Sun, H., Fan, Y.-L., Wang, A.-F., Zhao, R., Wang, W., and He, Y.-M. (2022c). "Study on the decay extent of wooden components of Danxia temple ancient building by polarized light fluorescence and X-Ray diffraction methods," *Cellulose Chemistry and Technology* 56(7-8), 717-726. DOI: 10.35812/CelluloseChemTechnol.2022.56.63

Yang, Y., Ji, H.-D., Li, B., Chen, L.-L., Song, X.-H., and Zhao, J. (2024). "Wood utilized for wooden components in ancient buildings of Tingbao Yang's former residence," *IAWA Journal.* DOI: 10.1163/22941932-bja10156

Zhang, D., Yu, Y.-Z., Guan, C., Wang, H., Zhang, H.-J., and Xin, Z.-B. (2021). "Nondestructive testing of defect condition of wall wood columns in Yangxin Hall of the Palace Museum, Beijing," *Journal of Beijing Forestry University* 43(5), 127-139. DOI: 10.12171/j.1000-1522.20210028

Article submitted: December 10, 2023; Peer review completed: April 23, 2024; Revised version received and accepted: April 25, 2024; Published: May 3, 2024.
DOI: 10.15376/biores.19.3.4087-4103